Journal of Sound and Vibration 332 (2013) 807–820

Contents lists available at SciVerse ScienceDirect

Journal of Sound and Vibration

journal homepage: www.elsevier.com/locate/jsvi

Model updating using antiresonant frequencies identified from transmissibility functions

V. Meruane*

Universidad de Chile, Department of Mechanical Engineering, Beaucheff 850, Santiago, Chile

ARTICLE INFO

Article history:
Received 30 November 2011
Received in revised form
3 April 2012
Accepted 19 October 2012
Handling Editor: I. Trendafilova
Available online 13 November 2012

ABSTRACT

Traditional model updating methods make use of modal information as natural frequencies and mode shapes. Natural frequencies can be accurately identified, but this is not the case for mode shapes. Mode shapes are usually accurate to within 10% at best, which can reduce the accuracy of the updated model. To solve this problem, some researchers have proposed antiresonant frequencies as an alternative to mode shapes. Antiresonances are identified easier and more accurately than mode shapes. In addition, antiresonances provide the same information as mode shapes and natural frequencies together. This article presents a new methodology to identify antiresonant frequencies from transmissibility measurements. A transmissibility function represents the relation in the frequency domain of the measured response of two points in the structure. Hence, it does not involve the measurement of excitation forces. These antiresonances are used to update the numerical models of two experimental structures: An 8-dof mass–spring system, and an exhaust system of a car. In both cases, the algorithm is tested first to update the numerical model of the structure, and second, to assess experimental damage.

1. Introduction

Model updating methods correlate a numerical model of a structure with its experimental data to improve the numerical model. In general, the numerical model is derived from finite element analysis (FEA) and the measurements are the vibration characteristics. The algorithm updates a set of parameters from the numerical model to obtain the minimum difference between the numerical and experimental data. Building an accurate numerical model, defining an appropriate parameterization, setting up the objective function and using a robust optimization algorithm are crucial factors in model updating.

One of the main challenges in model updating is the selection of an appropriate measure of the system response. This measure can be constructed in the time, frequency or modal domain. The last two are the most largely used. Traditional model updating methods make use of modal information as natural frequencies and mode shapes. Natural frequencies can be accurately identified, but this is not the case for mode shapes. Mode shapes are usually accurate to within 10% at best, which can reduce the accuracy of the updated model.

The idea of using directly the frequency response functions (FRFs) has attracted many researchers. Among all the dynamic responses, the FRF is one of the easiest to obtain in real-time, as the in-situ measurement is straightforward.

* Tel.: +56 2 9784597; fax: +56 2 689 6057.
E-mail address: vmeruane@ing.uchile.cl
URL: http://viviana.meruane.com

0022-460X/$ - see front matter © 2012 Elsevier Ltd. All rights reserved.
http://dx.doi.org/10.1016/j.jsv.2012.10.021

The advantage is that no modal extraction is necessary, thus contamination of the data with modal extraction errors is avoided. However, complex FRF data with noise can make the convergence process very slow and often numerically unstable as was found by Imregun et al. [1,2]. Furthermore, the success of the method is highly dependent on the selection of the frequency points. Lammens [3] addresses how a poor selection of the frequency points can lead to an unstable updating process and inaccurate results.

Frequency response functions have the disadvantage that they cannot be identified from output only modal analysis, thus the measurement of the excitation force is always required. For structures in real conditions, it often becomes very difficult to measure the excitation force. A critical issue in model updating is to reduce the dependence upon measurable excitation forces. Devriendt and Guillaume [4] presented an algorithm to identify modal parameters using transmissibility functions as primary data. Transmissibility functions relate the responses at two sets of coordinates. In consequence, it does not involve the measurement of excitation forces. The only condition is that the location of the excitation force must be known. The authors were able to correctly identify the system poles using transmissibility data. The proposed methodology has the advantage that the input force does not need to be white noise as required in classical operational modal analysis. This algorithm was later extended by Devriendt et al. [5] to identify also mode shapes using transmissibility measurements. Steenackers et al. [6] propose to use transmissibility measurements instead of frequency response functions in model updating. The researchers updated the finite element model of a mobile substation support structure using driving point transmissibility poles. Driving point transmissibility poles correspond to the resonances of the structure when the excitation degree of freedom is constrained. This is equivalent to the antiresonant frequencies of the driving point frequency response function. The authors conclude that the finite element model updated with transmissibility information is equivalent to the model updated with FRFs or operational modes. Hence, transmissibility functions are a good alternative in model updating when the excitation force is not measured. Maia et al. [7] presented a method for computing the transmissibility matrix from responses only. They showed that transmissibility functions are sensitive to damage, making them a possible approach for damage assessment. According to Johnson and Adams [8], since transmissibility depends only on the zeros (antiresonant frequencies) of the system, they are more sensitive to localize changes than methods using the system's poles (resonant frequencies). The authors successfully implemented an algorithm to localize damage using the changes on transmissibility functions. Although the use of transmissibility functions is recent, they seem to be quite promising in diverse fields as output-only modal analysis, model updating and damage assessment.

Recently, greatly attention has been given to the possible use of antiresonant frequencies in structural model updating. Antiresonances are an attractive alternative because they can be determined easier and with less error than mode shapes. Mottershead [9] showed that antiresonances sensitivities are linear combination of eigenvalues and mode shapes sensitivities. Hence, antiresonances are an alternative to natural frequencies and mode shapes since they provide the same information. As natural frequencies, antiresonances are located along the frequency axis and can be estimated from experimental FRFs more accurately than mode shapes. In addition, antiresonances can be identified from operational data [6,10]. Antiresonances are also very sensitive to small structural changes, which makes them good parameters for model updating. Antiresonances can be derived from point FRFs, where the response coordinate is the same as the excitation coordinate; or from transfer FRFs, where the response coordinate differs from the excitation coordinate. Point FRFs are preferred because matching problems arise when antiresonances from transfer FRFs are used. Moreover, small structural changes can modify significantly the distribution of the transfer antiresonances [11]. On the other hand, the procedure to obtain point FRFs differs from common modal testing, i.e. the excitation degree of freedom (dof) is moved together with the response dof. This may become not practical or too expensive. D'Ambrogio and Fregolent [11] updated the finite element model of a frame structure using resonant and antiresonant frequencies. With antiresonances from point FRFs the method is robust and leads to good results. In contrast, with transfer antiresonances the method is very unstable. Only with a careful selection of the updating parameter and a good match between experimental and numerical antiresonances they could reach results. Transfer antiresonances are used by Jones and Turcotte [12] to update a six meter flexible truss structure. The correctness of the updated model is studied by using it to detect damage. D'Ambrogio and Fregolent [13] updated the GARTEUR structure using an antiresonance-based method. The unmeasured point FRFs are synthesized through a truncated modal expansion. In a later work [14], they propose the use of zeros from a truncated expansion of the identified modes; they refer to these zeros as "virtual antiresonances". Results are compared with an updating method using MAC and natural frequencies. The updated models using either true or virtual antiresonances were more accurate than with MAC. Nam et al. [15] study the improvement in the performance of a parameter estimation algorithm by adding additional spectral information. The basic spectral information originates from the natural frequencies and the additional information from the antiresonances and static compliance dominant frequencies. Antiresonances are obtained from point and transfer FRFs. The authors evaluated the method with a numerical spring–mass system. They conclude that the accuracy of the algorithm can be improved with the use of additional spectral information as antiresonances and compliance dominant frequencies. Meruane and Heylen [16] show that antiresonances are a good alternative to mode shapes in model based damage assessment, but further research is needed in the identification and matching of experimental and numerical antiresonances. The use of antiresonances is still under development and the application of antiresonances to structural damage detection has not been fully investigated, mainly because the inverse optimization problem using antiresonances is very challenging and robust global optimization algorithms are needed. Nevertheless, Meruane and Heylen [16] demonstrated that Parallel Genetic Algorithms are robust enough to handle the difficult optimization problem of model updating using transfer antiresonances.

The present study proposes to identify antiresonance frequencies from the transmissibility functions. Antiresonance frequencies correspond to the dips in FRFs, and consequently to the dips and peaks in transmissibility functions. Hence, it is possible to identify antiresonance frequencies using transmissibility information. The main advantage of using transmissibility functions and not frequency response functions is that in the first case it is not necessary to measure the excitation force, which can be very challenging for structures in service. Nevertheless, the proposed approach has an important restriction in its application: there must be a single excitation force and its location must be known.

The problem of identifying antiresonances has never been tacked systematically. There are many algorithms available to identify resonance frequencies and mode shapes, but there is no validated algorithm to identify antiresonance frequencies. This study develops an algorithm capable to automatically identify antiresonance frequencies from transmissibility functions. This algorithm uses the rational fraction polynomials methodology proposed by Richardson and Formenti [17].

The model updating algorithm uses the optimization algorithm presented by Meruane and Heylen [16]. The objective function correlates antiresonant frequencies, and a Parallel Genetic Algorithm handles the inverse problem. The algorithm is evaluated with two experimental structures: An 8-dof mass–spring system, and an exhaust system of a car. In both cases, the algorithm is tested first to update the numerical model of the structure, and second, to assess experimental damage.

2. Transmissibility functions

Transmissibility functions are defined as the ratio in the frequency domain between two measured outputs:

$$T_{ij}^{k}(\omega)=\frac{X_{ik}(\omega)}{X_{jk}(\omega)} \tag{1}$$

where $X_{ik}(\omega)$ and $X_{jk}(\omega)$ are the output responses at degrees of freedom (dofs) i and j, due to an input force at dof k. In the case of a single force, the transmissibility functions only depend on the location of the force but not on the amplitude. Hence, the estimation of transmissibility functions does not involve the measurement of the excitation force. Frequency response functions (FRFs), on the other hand, require the measurement of the excitation force (F_k):

$$H_{ik}(\omega)=\frac{X_{ik}(\omega)}{F_{k}(\omega)} \tag{2}$$

$H_{ik}(\omega)$ is the FRF between the output dof i and the input dof k, when all the remaining dofs have zero inputs. Assuming a single input force at dof k, transmissibilities are related to the FRFs as

$$T_{ij}^{k}(\omega)=\frac{X_{ik}(\omega)}{X_{jk}(\omega)}=\frac{H_{ik}(\omega)F_{k}(\omega)}{H_{jk}(\omega)F_{k}(\omega)}=\frac{H_{ik}(\omega)}{H_{jk}(\omega)} \tag{3}$$

In practice, there are advantages in using alternative ways of calculating the transmissibility function using the auto- and cross-power spectrums:

$$T_{ij}^{k}(\omega)=\frac{X_{ik}(\omega)X_{jk}^{*}(\omega)}{X_{jk}(\omega)X_{jk}^{*}(\omega)} \tag{4}$$

where $X_{jk}^{*}(\omega)$ is the complex conjugate of $X_{jk}(\omega)$. The main reason for calculating the transmissibility functions with Eq. (4) and not with Eq. (1) is the reduction of uncorrelated noise.

3. Identification of antiresonant frequencies

3.1. Numerical antiresonances

For a lightly damped structure, antiresonant frequencies are almost unaffected by damping. Therefore, they can be obtained from the undamped system, using only the stiffness and mass matrices. The FRF matrix is by definition the inverse of the dynamic stiffness matrix:

$$\mathbf{H}(\omega)=\left(\mathbf{K}-\omega^{2}\mathbf{M}\right)^{-1}=\frac{\mathrm{adj}\left(\mathbf{K}-\omega^{2}\mathbf{M}\right)}{\det\left(\mathbf{K}-\omega^{2}\mathbf{M}\right)} \tag{5}$$

The operators adj(.) and det(.) indicate the adjoint and determinant respectively. Antiresonant frequencies correspond to the zeros of the FRFs. The zeros of the i, kth FRF are the values of ω for which the numerator of $H_{ij}(\omega)$ vanishes. The numerator of $H_{ij}(\omega)$ is the i, kth term of $\mathrm{adj}(\mathbf{K}-\omega^{2}\mathbf{M})$, which is given by $(-1)^{i+k}\det(\mathbf{K}_{i,k}-\omega^{2}\mathbf{M}_{i,k})$. The subscripts i, k denote that the ith row and kth column have been deleted. In consequence, the antiresonances of the i, kth FRF are the frequency values that satisfy:

$$\det\left(\mathbf{K}_{i,k}-\omega^{2}\mathbf{M}_{i,k}\right)=0 \tag{6}$$

This is equivalent to solve the eigenvalue problem:

$$(\mathbf{K}_{i,k}-\omega^2\mathbf{M}_{i,k})\mathbf{u}=0 \tag{7}$$

If $i=k$ Eq. (7) represents a physical system obtained by grounding the ith degree of freedom. Therefore, the antiresonant frequencies obtained from point FRFs ($i=k$) are equivalent to the resonant frequencies of the structure with the ith degree of freedom grounded.

If $i\neq k$ Eq. (7) does not represent any physical system and some of the eigenvalues may be negative or complex, these values must not be considered as antiresonant frequencies.

3.2. Experimental antiresonances

The proposed algorithm identifies antiresonances using rational fraction polynomials [17]. The FRFs and/or the transmissibility functions are represented in a rational fraction form. This representation is the ratio of two polynomials, where the orders of the numerator and denominator are independent of one another. A FRF is represented in a rational fraction form as follows:

$$H_{ik}(\omega)=\frac{N_{ik}(\omega)}{D(\omega)}=\frac{\sum_{p=1}^{n}a_p s^p}{\sum_{p=1}^{m}b_p s^p} \tag{8}$$

The denominator of the fraction, $D(\omega)$, is the characteristic polynomial of the system, which is common for all the FRFs. The zeros of this polynomial correspond to the system poles (resonant frequencies). Similarly, the roots of the numerator polynomial, $N_{ik}(\omega)$, are the zeros of the i, kth FRF, i.e. the antiresonant frequencies. Hence by curve fitting Eq. (8) to the FRF data, and then solving the roots of both polynomials, the resonant and antiresonant frequencies of the system can be determined. On the other hand, a transmissibility function is represented as

$$T_{ij}^{k}(\omega)=\frac{H_{ik}(\omega)}{H_{jk}(\omega)}=\frac{N_{ik}(\omega)}{N_{jk}(\omega)}=\frac{\sum_{p=1}^{n}a_p s^p}{\sum_{p=1}^{m}c_p s^p} \tag{9}$$

The zeros of the numerator polynomial correspond to the antiresonant frequencies of the i, kth FRF, while the zeros of the denominator polynomial correspond to the antiresonant frequencies of the j, kth FRF. Thus, transmissibility functions only contain information only about the antiresonant frequencies. By curve fitting the transmissibility functions to Eq. (9) and solving the roots of both polynomials it is possible to determine the antiresonant frequencies of the system for a given excitation location.

To determine the antiresonant frequencies of the j, kth FRF, more accurately, the proposed algorithm uses the summation of the amplitudes of all measured transmissibility functions whose denominators are the response in j. This function is calculated as:

$$T_j^k(\omega)=\sum_{p=1,p\neq j}^{N}\left|\mathrm{Re}(T_{pj}^k(\omega))\right|+j\sum_{p=1,p\neq j}^{N}\left|\mathrm{Im}(T_{pj}^k(\omega))\right| \tag{10}$$

where N is the number of responses measured. The superscript k indicates de location of the excitation and the subscript j indicates location of the response. Summing the transmissibility functions helps to reduce the noise to signal ratio, and hence to increase the accuracy of the detected antiresonances. The resulting function, $T_j^k(\omega)$, contains only peaks at the antiresonance frequencies of the j, kth FRF. Hence, by curve fitting the absolute value of $T_j^k(\omega)$ to a rational fraction form and solving the roots of the denominator, the antiresonances of the j, kth FRF are identified.

The curve fitting process uses the algorithm proposed by Richardson and Formenti [17] with orthogonal Forsythe polynomials. A stabilization diagram assists in separating physical poles from mathematical poles [18]. The algorithm uses the same order for the numerator and denominator. The following stabilization criterion is used: 1% for frequency stability and 5% for damping stability.

Figs. 1 and 2 illustrate the antiresonance identification process for an eight dof system, which is formed by eight translating masses connected by springs as shown in Fig. 5. In this example, the location of the excitation is dof 1, and the dofs where the antiresonances are being identified are 1, 5 and 8. Fig. 1 illustrates the identification process using FRFs; the FRFs measured at degrees of freedom 1, 5 and 8 are plotted together with their corresponding stabilization diagram. The order on the left Y-axis corresponds to the order of the fitted orthogonal polynomials. The 'x's and circles correspond to the roots of the numerator polynomial; a circle indicates a stable root. Here, the algorithm automatically identifies an antiresonance if there are more than 10 stable roots in a row. Note that as the response location gets away from the point of excitation, the number of antiresonant frequencies diminishes. In the farthest point (dof 8) there are no antiresonant frequencies, as shown in Fig. 1. Therefore, this dof does not provide information for the current model updating algorithm.

Fig. 2 illustrates the identification process using the summation of transmissibility functions as defined in Eq. (10), this summation is computed using transmissibilities between all measured degrees of freedom (1–8). The transmissibility sums, $T_1^1(\omega)$, $T_5^1(\omega)$ and $T_8^1(\omega)$, are plotted together with their corresponding stabilization diagram. The 'x's and circles correspond to the roots of the denominator polynomial; a circle indicates a stable root.

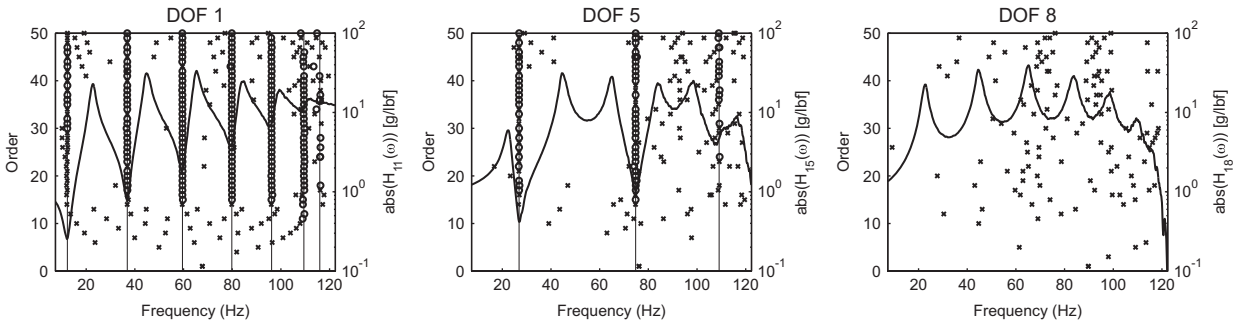

Fig. 1. Identification of antiresonant frequencies using frequency response functions.

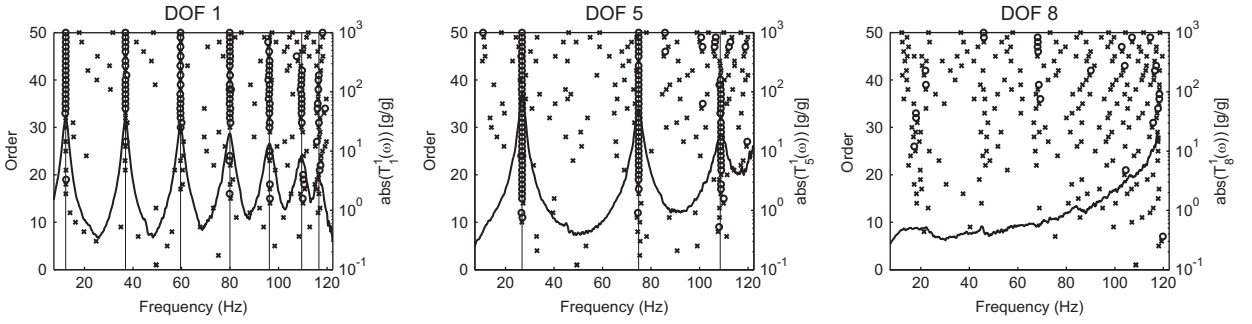

Fig. 2. Identification of antiresonant frequencies using summation of transmissibility functions.

The results show that the antiresonances identified using frequency response functions or transmissibility functions are the same; the differences are lower than 0.5%. In consequence, the accuracy in the antiresonance identification process is the same for FRFs or transmissibility functions, even though the excitation force is not measured in the second case. Furthermore, there are some antiresonant frequencies that are easier to identify in the transmissibility case. For example, in the first dof the antiresonance at 116 Hz is much clear in the sum of transmissibility functions than in the FRF.

4. Model updating algorithm.

4.1. Formulation of the optimization problem

Defining β_i as the ith updating parameter, the model updating problem is a constrained nonlinear optimization problem, where $\boldsymbol{\beta}=\{\beta_1, \beta_2,\ldots, \beta_n\}$ are the optimization variables. The objective function correlates antiresonant frequencies. The error in antiresonances is represented by the ratio between the experimental and analytical antiresonances,

$$\varepsilon_{i,n}(\boldsymbol{\beta}) = \frac{\omega^A_{r,i,n}(\boldsymbol{\beta})^2}{\omega^{E\ 2}_{r,i,n}} - 1 \tag{11}$$

The superscripts A and E refer to analytical and experimental, $\omega_{r,i,n}$ is the ith antiresonance of the nth dof. The objective function is given by

$$J\left(\boldsymbol{\beta}\right) = \sum_n \sum_i \left\| \varepsilon_{r,i,n}(\boldsymbol{\beta}) \right\| \tag{12}$$

The optimization problem is defined as

$$\begin{aligned} &\min && J(\boldsymbol{\beta}) \\ &\text{subject to} && lb_i \le \beta_i \le ub_i \end{aligned} \tag{13}$$

where lb_i and ub_i are the lower and upper bounds of the ith updating parameter.

4.1.1. Special case: damage assessment

The purpose of damage assessment is to detect and characterize damage at the earliest possible stage. The basic idea of vibration-based damage assessment is that the vibration characteristics (natural frequencies, mode shapes, damping, frequency response function, etc.) are functions of the physical properties of the structure. Thus, changes to the material and/or geometric properties due to damage will cause detectable changes in the vibrations characteristics. Many studies

have demonstrated that vibration measurements are sensitive enough to detect damage even if it is located in hidden or internal areas [19]. Once the vibration characteristics of the structure have been measured, the damage assessment algorithm attempts to solve the inverse problem: to assess which damage is producing the measured changes in the vibration characteristics. This is a model-updating problem, in which the differences between models of the structure correlated before and after the presence of damage are used to localize and determine the extent of the damage.

Damage is represented by an elemental stiffness reduction factor β_i, defined as the ratio between the stiffness reduction to the initial stiffness. This is the simplest method to model damage. Although this model has problems in matching damage severity to crack depth and is affected by mesh density, Friswell and Penny [20] demonstrate that at low frequencies this method can correctly model a crack. It is shown that a more detailed model does not substantially improve the results from damage assessment. The stiffness matrix of the damaged structure $\mathbf{K}_d$ is expressed as a sum of element matrices multiplied by reduction factors [16]

$$\mathbf{K}_d = \sum_i (1-\beta_i)\mathbf{K}_i \tag{14}$$

The value $\beta_i=0$ indicates that the element is undamaged whereas $0<\beta_i\leq 1$ implies partial or complete damage.

The objective function is the same as in Eq. (12), but a damage penalization function, $F_{D,}$ is added:

$$J(\boldsymbol{\beta}) = \sum_n \sum_i \|\varepsilon_{r,i,n}(\boldsymbol{\beta})\| + F_D \tag{15}$$

As demonstrated by Meruane and Heylen [16], damage penalization helps to avoid falsely detected damages because of experimental noise or numerical errors. Two damage penalization functions are used:

$$F_{D,1} = \gamma_1 \sum_i \beta_i$$

$$F_{D,2} = \gamma_2 \sum_i \delta_i, \quad \delta_i = \begin{cases} 1 & \beta_i > 0 \\ 0 & \beta_i = 0 \end{cases} \tag{16}$$

The first penalizes the total amount of damage. The second, on the other hand, penalizes the number of damage locations. Depending on the damage pattern expected one can use the first function, the second or a combination of both. The value of the constants γ_1 and γ_2 depend on the confidence in the numerical model and the experimental data. According to the results obtained in [16], a good value for γ_1 and γ_2 is 0.1. Here, F_D is defined as

$$F_D = F_{D,1} + F_{D,2}, \text{ with } \gamma_1 = \gamma_2 = 0.1 \tag{17}$$

The results obtained with the proposed approach are compared with the ones obtained using a conventional approach based on mode shapes and natural frequencies. The objective function is defined as follows:

$$J(\boldsymbol{\beta}) = \sum_i \left\| \frac{\omega_{A,i}(\boldsymbol{\beta})^2}{\omega_{E,i}{}^2} - 1 \right\| + \sum_i \left(1 - MAC(\phi_{A,i}, \phi_{E,i})\right)^2 + F_D \tag{18}$$

The subscripts A and E refer to analytical and experimental respectively, ω_i is the ith resonant frequency and $\phi_{A,i}$ is the ith mode shape. Modal Assurance Criterion (MAC) is a factor that expresses the correlation between two modes. A value of 0 shows no correlation whereas a value of 1 shows two completely correlated modes. This objective function is selected to compare the performance of the proposed approach because it was the one that provided the best performance in the study presented by Meruane and Heylen [21].

4.2. Optimization algorithm

Here the optimization is particularly challenging and a robust optimization algorithm is needed. Having this in consideration it is proposed to work with Genetic Algorithms (GAs) has an optimization tool. The GA is a global searching process based on Darwin's principle of natural selection and evolution. A sequential GA consists of three main operations: selection, genetic operations and replacement (see Fig. 3). The GA starts with creating a random initial population. A set of possible solutions, referred to as chromosomes, form the initial population. A sequence of genes that represents the variables of the problem forms each chromosome. The fitness function evaluates the fitness of each chromosome. Next, the algorithm passes the initial population through a selection process. Chromosomes with a higher fitness have a higher probability to survive in the next generation. After the selection process, the chromosomes are randomly paired. Each pair of chromosomes is referred to as parents. The algorithm uses the basic GA operators, crossover and mutation, to reproduce the parents. As a result, it creates new pairs of children. Crossover and mutation are applied randomly with a probability of p_c and p_m respectively. After the process of selection, genetic operations and replacement, the algorithm evaluates the new population. This process is iterated for a number of generations until a convergence criterion is achieved. The crossover is considered the main search operator. Each crossover technique directs the search in different areas near the parents, some of them use more exploration (or interpolation) and others more exploitation (or extrapolation). For the algorithm to be successful there must be an adequate balance between exploration and exploitation. Herrera et al. [22] show that by combining different types of crossovers the effectiveness of the search is improved.

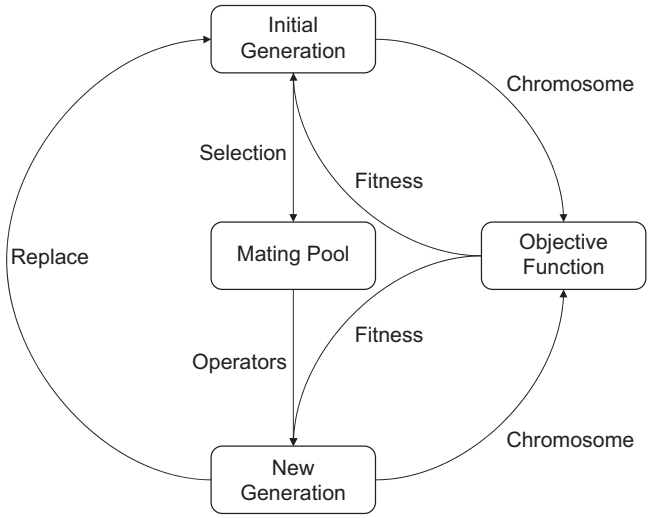

Fig. 3. Working principle of a sequential Genetic Algorithm.

The problem with sequential GAs is that they are inherently slow when they work with complicated or time consuming objective functions. To improve the searching speed, Parallel Genetic Algorithms (PGAs) are proposed. PGAs are particularly easy to implement and provide a superior numerical performance. PGAs are not just a parallel version of GAs. In addition to being faster than sequential GAs, they lead to better results. Many studies show that with PGAs the execution time can be reduced by a factor greater than the number of processors used [23]. The basic idea in parallel processing is to divide a large problem into smaller tasks. A group of processors solves these tasks simultaneously. Parallelization is applied to GA by different approaches, three main methods are distinguished: global, migration and diffusion. Migration GAs, also known as multiple population GAs, are the most popular parallel method and potentially the most efficient. In this case, a number of populations are running in parallel. Each population runs a conventional GA individually. These populations exchange their individuals occasionally. This exchange is denominated migration. The separation into sub-populations prevents premature convergence because it allows each population to search in different zones. Meruane and Heylen [24] investigated the advantages of PGAs in a structural damage detection problem. They concluded that PGAs always provide an improved and faster search in the solution space compared to sequential GAs.

Fig. 4 illustrates the optimization algorithm used here. The algorithm employs a multiple population GA with four populations and a neighborhood migration. Each population runs a sequential GA that from time to time exchanges information with its neighbors (migration). The gene of each chromosome is an updating parameter of the optimization problem. The GA uses a normalized geometric selection. To ensure an effective search with an adequate balance between exploration and exploitation, each population works with a different crossover, being the following ones: arithmetic crossover, heuristic crossover, BLX-0.5 crossover and uniform crossover. In addition, each population applies both boundary and uniform mutations. Each population has a size of 40 individuals and the crossover and mutation probabilities are $p_c=0.80$ and $p_m=0.02$ respectively.

The migration interval is automatically adjusted. If a population has no improvement after 40 generations, the GA stops and exchanges the individuals with their neighbors. This exchange of individuals is synchronous i.e., the algorithm waits until the five populations are ready to perform the migration. At each migration, each population sends its best individual, whereas the received individual replaces its worse individual. Before each migration, the algorithm compares the best individuals from all populations, if they are all the same the optimization is finished.

During the optimization process the algorithm must match correctly each experimental antiresonance with an experimental one. This becomes a difficult task, mainly because the antiresonances distribution is significantly altered with small structural changes. Nevertheless, since the optimization algorithm used here is not gradient based, a perfect matching is not necessary. Moreover, the matching can change at each step and the optimization is not affected. Having this in consideration, the numerical and experimental antiresonances are paired each time the objective function is evaluated. Each experimental antiresonance is paired with the closest numerical one. Because the number of experimental and numerical antiresonances may not be the same, a numerical antiresonance is allowed to be paired with one or more experimental antiresonances.

5. Application cases

5.1. 8 dof mass–spring system

The structure consists of an eight dof spring–mass system. Los Alamos National Laboratory (LANL) designed and constructed this system to study the effectiveness of various vibration-based damage identification techniques.

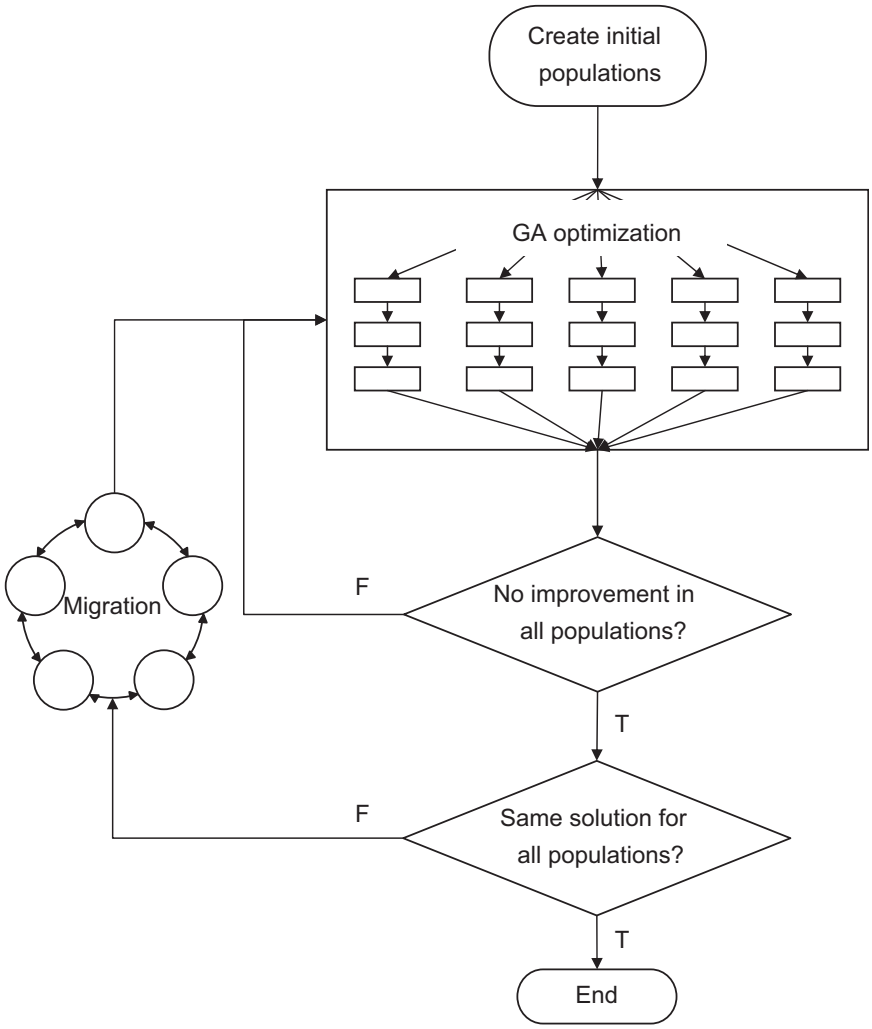

Fig. 4. Parallel optimization algorithm.

As shown in Fig. 5, eight translating masses connected by springs form the system. Each mass is a disc of aluminum with a diameter of 76.2 mm and a thickness of 25.4 mm. The masses slide on a highly polished steel rod, and are fastened together with coil springs. Springs and mass locations are designated sequentially with the first ones the closest to the shaker attachment.

In the undamaged configuration all springs are identical and have a linear spring constant. Damage is simulated by replacing the fifth spring with another spring that has a lower stiffness. Acceleration is measured horizontally at each mass, giving a total of eight measured dof. The structure is excited randomly by an electrodynamic shaker. The responses are measured in the 8 dofs in the undamaged and damaged cases.

5.1.1. Model updating

The finite element model was built in Matlab; the initial parameters are the following:

- Mass 1: 559.3 g
- Masses 2–8: 419.4 g
- Spring constants: 56.7 kN m^{-1}

During the model updating process, the masses and spring constants were updated individually. It was allowed a variation of 10% with respect to their initial values. Twenty-eight antiresonances were identified from the transmissibility functions, all of them are used to update the model.

Fig. 6(a) shows an example of a transmissibility function before and after updating the numerical model. After updating, the numerical model is much closer to the experimental one. Fig. 6(b) shows the difference between the

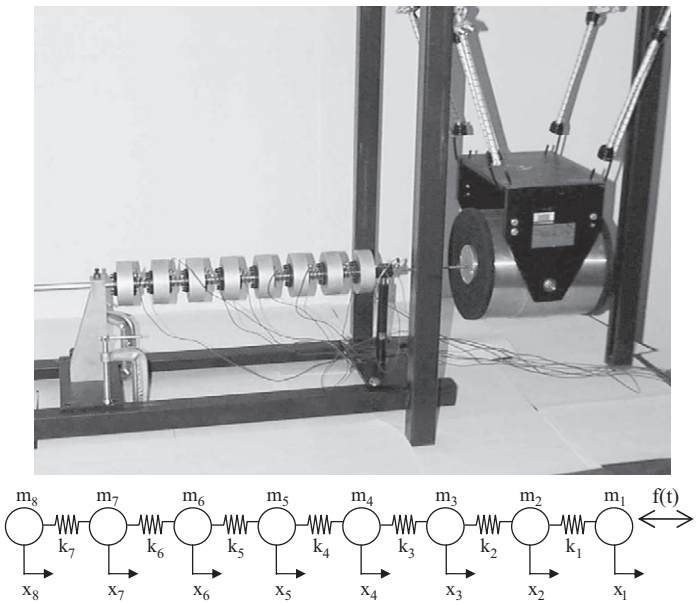

Fig. 5. Experimental 8 degrees of freedom system.

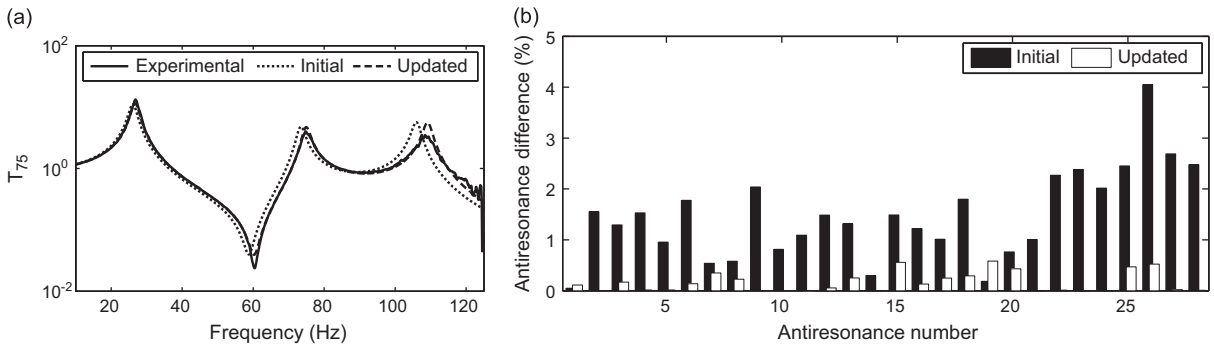

Fig. 6. (a) Transmissibility function T_{7-5} and (b) antiresonance difference before and after updating the numerical model.

numerical and experimental antiresonances before and after updating. The maximum difference between the experimental and numerical antiresonances before updating is 4%, whereas after updating is only 0.58%.

5.1.2. Damage assessment

After model updating, a damage assessment case evaluates the accuracy of the numerical model and model-updating algorithm. In this case, the expected values for the updating parameters are known. This study has two primary purposes: First, to verify that the updated numerical model is accurate, and second to evaluate that the algorithm is able to find and correct the actual differences between the numerical and experimental models.

Experimental damage is simulated by reducing the stiffness of the fifth spring in 55%. During the model updating the stiffness of the eight springs were updated individually, according to the procedure described in Section 4.1.1. Fig. 7 illustrates a transmissibility function before and after model updating. The results show that after updating, the numerical model is much closer to the experimental one. It should be noted that this updating algorithm is almost unaffected by the experimental noise, because even in the presence of experimental noise antiresonances are accurately identified.

Fig. 8 shows the reduction of stiffness detected with the current approach and with an approach based on mode shapes and natural frequencies. The results in both cases are very accurate, although with antiresonant frequencies, quantification is more accurate; the error is lower than 0.5%. The algorithm does not detect damage in other springs than the fifth, thanks to the damage penalization strategy adopted.

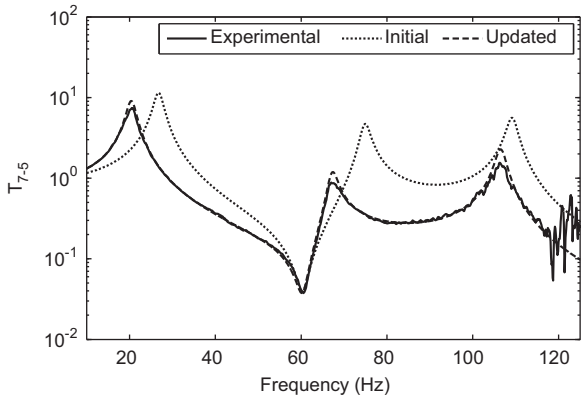

Fig. 7. Transmissibility function T_{7-5} before and after updating the numerical model.

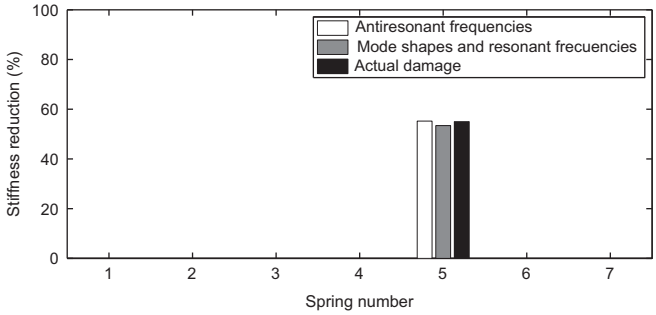

Fig. 8. Reduction of stiffness detected with antiresonant frequencies or with mode shapes and resonant frequencies, compared to the actual damage.

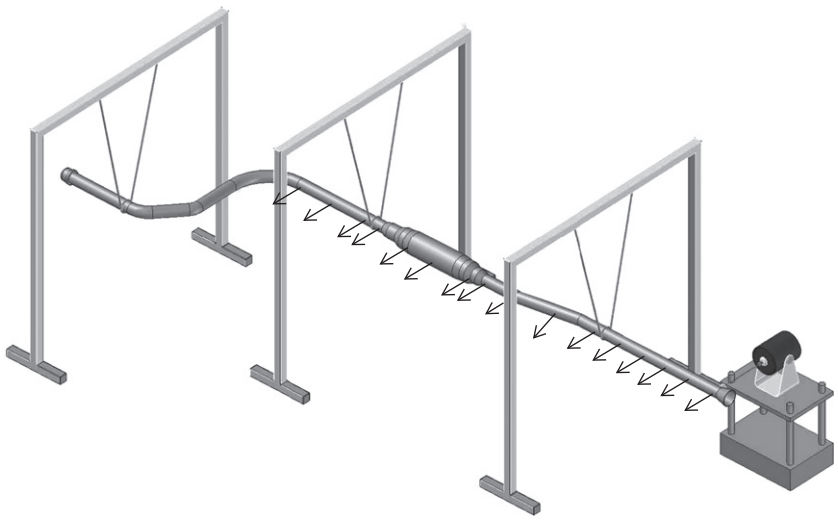

Fig. 9. Experimental set-up.

5.2. Car exhaust system

The structure consists of a car exhaust system as shown in Fig. 9. The dimensions are: length: 2.3 m, width: 0.45 m. The exhaust pipe has a diameter of 38 mm. The structure is suspended by soft springs and it is excited randomly by an electrodynamic shaker. The response is captured by 16 accelerometers. The test is performed in a frequency range of 0–512 Hz with a frequency resolution of 0.25 Hz.

5.2.1. Model updating

The numerical model shown in Fig. 10 is built in Matlab with 2D beam elements and concentrated inertias for the masses. The model has 47 beam and 5 inertia elements, with 144 dof. Generic material properties are used.

The updating parameters are the following: the thickness and material properties in the different sections of the tube, the mass of the five concentrated inertias, and the rotation angle of some elements. There are a total of 21 updating parameters. Thirty-two antiresonances were identified from the transmissibility functions, all of them are used during the model updating process.

Fig. 11(a) shows an example of a transmissibility function before and after model updating. After updating, the numerical model is much closer to the experimental one. Fig. 11(b) shows the difference between the numerical and experimental antiresonances before and after updating. The maximum difference between the experimental and numerical antiresonances before updating is 38.5%, whereas after updating is 7.6%.

5.2.2. Damage assessment

As described by Meruane and Heylen [16], a single fatigue crack with three increasing levels of damage is introduced to the structure. Fig. 12(a) shows the crack, which is located in element 31 close to the welded connection between elements 30 and 31 (see Fig. 10) and covers around 60% of the pipe perimeter. The fatigue test is done again twice to grow the crack. Fig. 12(b) shows the second damage level; here the structure has already failed due to unstable crack propagation. The open crack covers around 70% of the perimeter. The last damage level is shown in Fig. 12(c), the crack covers around 85% of the perimeter.

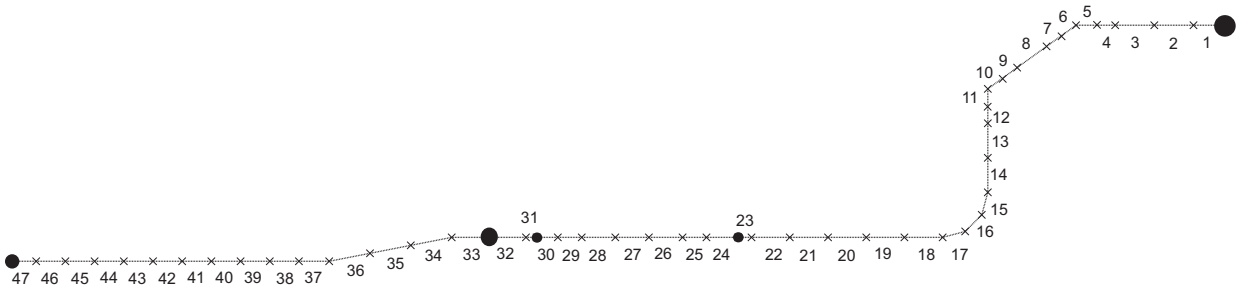

Fig. 10. Finite element model and element numbering.

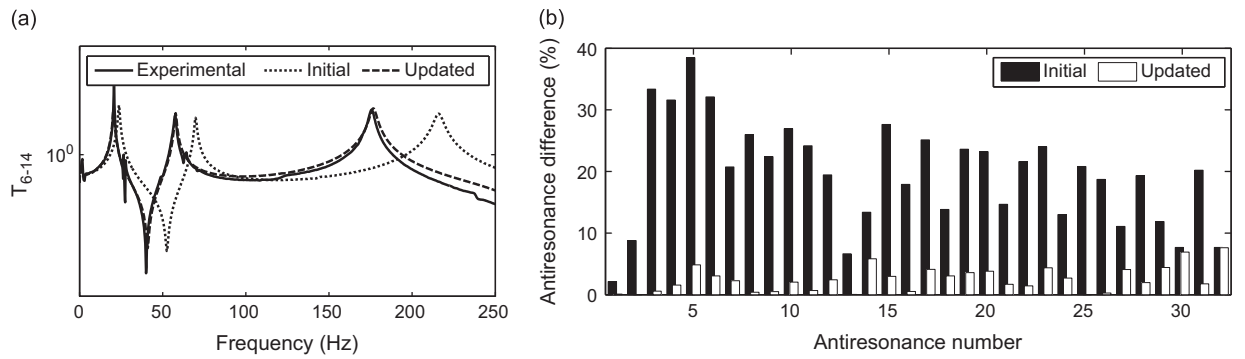

Fig. 11. (a) Transmissibility function T_{6-14} and (b) antiresonance difference before and after updating the numerical model.

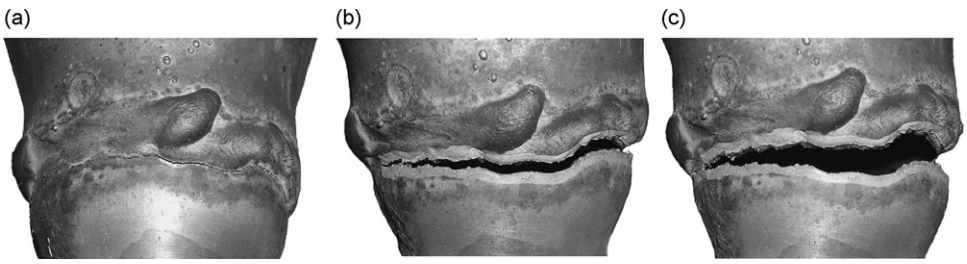

Fig. 12. Three levels of damage introduced to the structure.

Elements 18–47 are considered possible locations of damage, giving 30 stiffness reduction factors to be updated. All the identified antiresonances in the range 0–260 Hz from the 16 measured dofs are used. The number of identified antiresonances varies from 32 to 36 depending on the case. Fig. 13 shows the improvement in one of the numerical

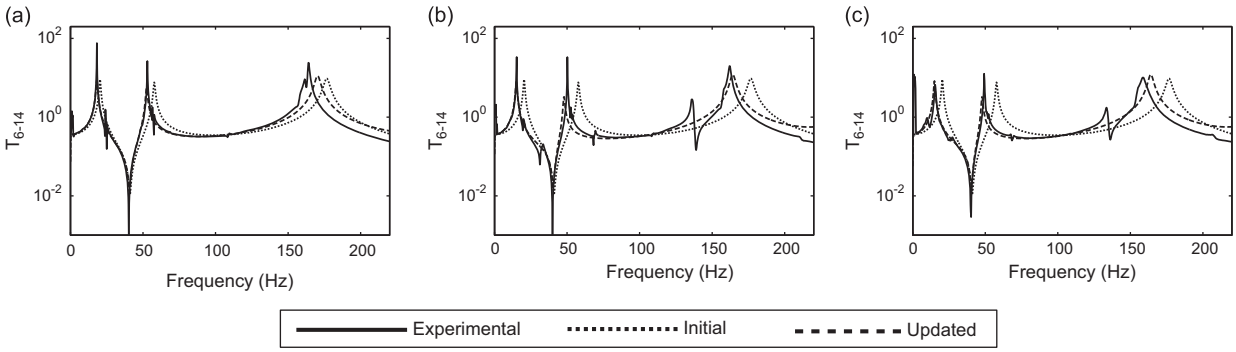

Fig. 13. Transmissibility function T_{6-14} before and after updating the numerical model in the three damaged cases.

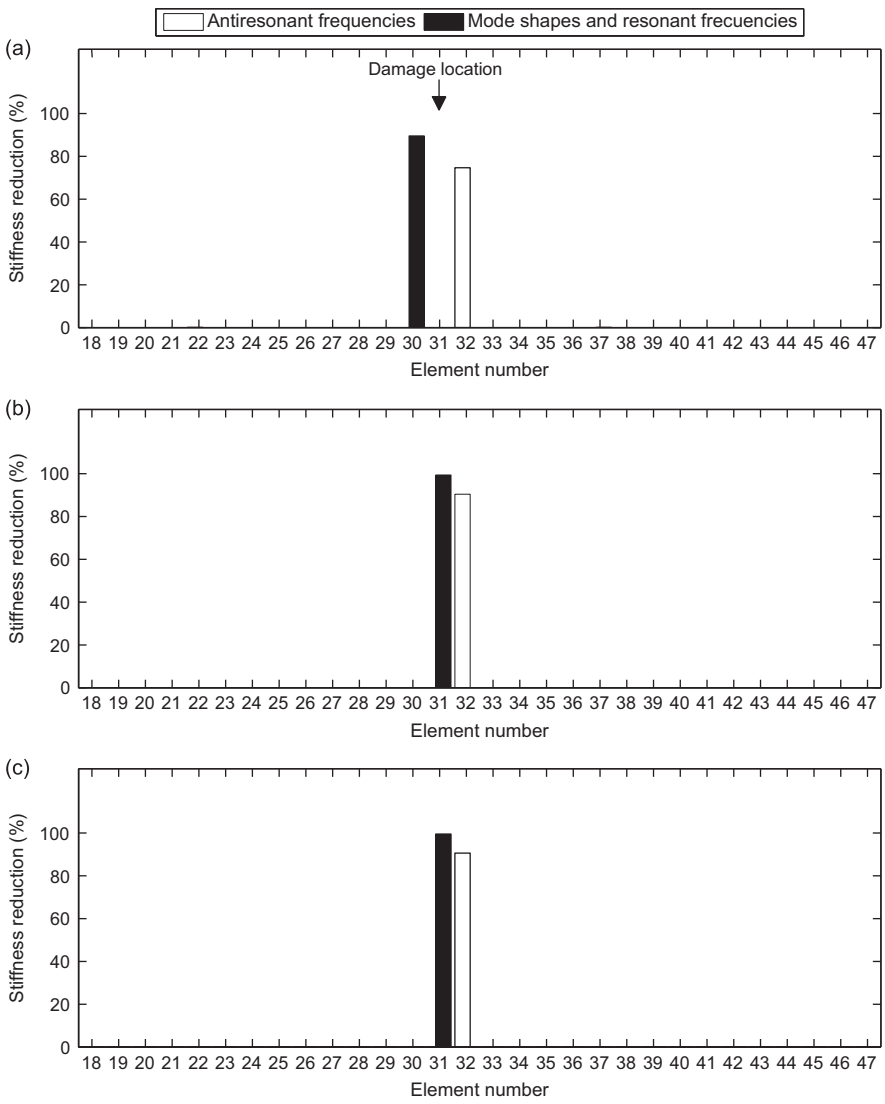

Fig. 14. Reduction of stiffness detected with both approaches.

Table 1
Damage detected on each case.

Case	Antiresonant frequencies		Mode shapes and resonant frequencies	
	Element	Damage %	Element	Damage %
1	32	74.7	30	89.6
2	32	90.4	31	99.4
3	32	90.6	31	99.5

transmissibility functions after updating. In the three cases, the numerical model gets much closer to the experimental one after updating.

Fig. 14 illustrates the reduction of stiffness detected on each case, using antiresonant frequencies or mode shapes and resonant frequencies. These results are summarized in Table 1.

With the current approach, damage is detected only in element 32, which is close to the experimental damage (element 31). The reduction of stiffness detected on each case is 75%, 90% and 91% respectively. Hence, the magnitude of the detected damage increases with an increment of the experimental damage. With the approach based on mode shapes and resonant frequencies, the damage detected is closer to the actual damage location. In addition, the magnitude of the detected damage is larger than the one detected with the first approach. This is explained by the fact that the damage detected is closer to the actual location. Nevertheless, both approaches have detected damage very close to actual location and the quantification is reasonable. The results from the first approach can be improved by adding more measuring points close to the damaged area.

6. Conclusions

This article presents a new methodology to identify antiresonant frequencies from transmissibility functions. These antiresonances are used in a model-updating algorithm. A parallel Genetic Algorithm handles the optimization problem. The objective function correlates experimental and numerical antiresonant frequencies. Two experimental cases verify the algorithm: An 8 dof mass–spring system, and an exhaust system of a car. In both cases, the model updating algorithm is tested first to update the numerical model, and second, to assess experimental damage. In the case of damage assessment, the algorithm uses the damage penalization technique proposed by Meruane and Heylen [16] to avoid falsely detected damages.

The results demonstrate that antiresonant frequencies can be identified from transmissibility functions, as easily as, resonant frequencies are identified from frequency response functions. Nevertheless, antiresonant frequencies have two principal advantages. First, it is not necessary to measure the excitation force, and second, they contain more information than resonant frequencies. For example, in the case of damage assessment, resonant frequencies contain information only about the amount of damage [25], while antiresonant frequencies contain information regarding the amount and location.

In both application cases, the algorithm is successful in updating the numerical models. In the cases of damage assessment, the damage detected has a good correspondence with the experimental damage. The results demonstrate that it is possible to accurately locate and quantify structural damage using only antiresonance information obtained from transmissibility functions. Hence, antiresonant frequencies are a very attractive feature, which can be extracted from output-only data, to be used in model updating and damage assessment.

Acknowledgments

This research has been partially funded by Program U-INICIA VID 2011, Grant U-INICIA 11/01, University of Chile and by the fondo nacional de desarrollo científico y tecnológico of the Chilean government, proyect Fondecyt iniciación 11110046.

References

[1] M. Imregun, W.J. Visser, D.J. Ewins, Finite element model updating using frequency response function data I. Theory and initial investigation, *Mechanical Systems and Signal Processing* 9 (2) (1995) 187–202.
[2] M. Imregun, K.Y. Sanliturk, D.J. Ewins, Finite element model updating using frequency response function data II. Case study on a medium-size finite element model, *Mechanical Systems and Signal Processing* 9 (2) (1995) 203–213.
[3] S. Lammens, Frequency Response Based Validation of Dynamic Structural Finite Element Models, PhD Dissertation, Katholieke Universiteit Leuven, Leuven, 1995.
[4] C. Devriendt, P. Guillaume, Identification of modal parameters from transmissibility measurements, *Journal of Sound and Vibration* 314 (1–2) (2008) 343–356.
[5] C. Devriendt, G. Steenackers, G. De Sitter, P. Guillaume, From operating deflection shapes towards mode shapes using transmissibility measurements, *Mechanical Systems and Signal Processing* 24 (3) (2010) 665–677.
[6] G. Steenackers, C. Devriendt, P. Guillaume, On the use of transmissibility measurements for finite element model updating, *Journal of Sound and Vibration* 303 (3–5) (2007) 707–722.
[7] N.M.M. Maia, J.M.M. Silva, A.M.R. Ribeiro, The transmissibility concept in multi-degree-of-freedom systems, *Mechanical Systems and Signal Processing* 15 (1) (2001) 129–137.

[8] T.J. Johnson, D.E. Adams, Transmissibility as a differential indicator of structural damage, *Journal of Vibration and Acoustics* 124 (4) (2002) 634–641.
[9] J.E. Mottershead, On the zeros of structural frequency response functions and their sensitivities, *Mechanical Systems and Signal Processing* 12 (5) (1998) 591–597.
[10] D. Hanson, T.P. Waters, D.J. Thompson, R.B. Randall, R.A.J. Ford, The role of anti-resonance frequencies from operational modal analysis in finite element model updating, *Mechanical Systems and Signal Processing* 21 (1) (2007) 74–97.
[11] W. D'Ambrogio, A. Fregolent, The use of antiresonances for robust model updating, *Journal of Sound and Vibration* 236 (2) (2000) 227–243.
[12] K. Jones, J. Turcotte, Finite element model updating using antiresonant frequencies, *Journal of Sound and Vibration* 252 (4) (2002) 717–727.
[13] W. D'Ambrogio, A. Fregolent, Results obtained by minimizing natural frequency and antiresonance errors of a beam model, *Mechanical Systems and Signal Processing* 17 (1) (2003) 29–37.
[14] W. D'Ambrogio, A. Fregolent, Dynamic model updating using virtual antiresonances, *Shock and Vibration* 11 (3–4) (2004) 351–363.
[15] D. Nam, S. Choi, S. Park, N. Stubbs, Improved parameter identification using additional spectral information, *International Journal of Solids and Structures* 42 (18–19) (2005) 4971–4987.
[16] V. Meruane, W. Heylen, Structural damage assessment with antiresonances versus mode shapes using parallel genetic algorithms, *Structural Control & Health Monitoring* 18 (8) (2011) 825–839.
[17] M.H. Richardson, D.L. Formenti, Parameter estimation from frequency response measurements using rational fraction polynomials, *Proceedings of the First International Modal Analysis Conference*, 1982, pp. 167–181.
[18] H. Van der Auweraer, B. Peeters, Discriminating physical poles from mathematical poles in high order systems: use and automation of the stabilization diagram, *Proceedings of the Instrumentation and Measurement Technology Conference, IMTC/2004*, Vol. 3, 2004, pp. 2193–2198.
[19] Y.J. Yan, L. Cheng, Z.Y. Wu, L.H. Yam, Development in vibration-based structural damage detection technique, *Mechanical Systems and Signal Processing* 21 (5) (2007) 2198–2211.
[20] M.I. Friswell, J.E.T. Penny, Crack modeling for structural health monitoring, *Structural Health Monitoring* 1 (2) (2002) 139–148.
[21] V. Meruane, W. Heylen, An hybrid real genetic algorithm to detect structural damage using modal properties, *Mechanical Systems and Signal Processing* 25 (2011) 1559–1573.
[22] F. Herrera, M. Lozano, A.M. Sanchez, Hybrid crossover operators for real-coded genetic algorithms: an experimental study, *Soft Computing—A Fusion of Foundations, Methodologies and Applications* 9 (4) (2005) 280–298.
[23] W.F. Punch, How effective are multiple populations in genetic programming, *Genetic Programming* 98 (1998) 308–313.
[24] V. Meruane, W. Heylen, Damage detection with parallel genetic algorithms and operational modes, *Structural Health Monitoring* 9 (6) (2010) 481–496.
[25] O.S. Salawu, Detection of structural damage through changes in frequency: a review, *Engineering Structures* 19 (9) (1997) 718–723.